**Magnetic Delay Transformer (MDT)**

## 1. Introduction.

There is interest in using the magnetic delay characteristics of transformer cores as a means of accessing the zero point energy (zpe) of space. This line of enquiry was initiated by Prof. Turtur's paper which suggested that EM radiation (actually antenna near-field radiation in his example) was evidence of zpe and that some zpe could be captured using delay techniques. It is perhaps unfortunate then that his proposed capacitance-loaded magnetic motor did not use magnetic delay techniques and is doomed to failure. In this present paper a transformer is represented by a magnetic circuit having dynamic characteristics as described in my previous paper "Analysing Transformers in the Magnetic Domain". That analysis is extended to take account of the finite magnetic propagation delay by modelling the magnetic circuit as a transmission line. It was shown in my recent paper "Transformer Core as a Transmission Line" that, using classical transmission line theory, a line with reactive $Z_0$ when terminated with a reactive $Z$ can exhibit a negative value of input resistance. By applying that classical theory to the magnetic domain circuit, this present paper shows that a capacitively loaded transformer could also exhibit negative input resistance.

The magnetic domain model has been used to predict the characteristics of a transformer using a ferrite ring core where measurements of an actual transformer have been performed. As previously reported in my paper "Comparison of MDT Measurements with Magnetic Domain Transmission-Line Analysis" the initial model correctly reproduced the input impedance over the frequency band covering LC resonance, but whereas the model then showed the input resistance going negative at a higher frequency, the measured results did not show this trend. Various attempts were made to introduce losses into the model that would account for the measured results. It was discovered that the measurements could only be reproduced if losses were included in the leakage flux path. By trial and error it was determined that the complex permeability $\mu''$ associated with these losses could not come from the core characteristics, but were a separate feature where $\mu''$ is directly proportional to frequency. It is believed that this loss feature is unknown in transformers and could be an important discovery. It seems likely that the losses are due to radiation, so would not be prominent in low frequency transformers, but here where we have frequencies above 1MHz their effect is to hide the potential for self oscillation. It is hoped that reducing the flux leakage by introducing a conductive screen will bring the negative input resistance into focus.

## 2. MDT as Measured.

The MDT measurements were those taken by Graham on a single 3F4 ferrite core having 6 turns primary and secondary, see Figure 1. The secondary was loaded with resistor values ranging from 10M ('scope probe) down to 1K shunted by capacitor values ranging from 10pF ('scope probe) up to 500pF. Input voltage, current, and phase angle were measured over a frequency range from 100KHz to 20MHz. From these measurements the input impedance has been calculated for comparison with values obtained from analysis. Output voltage and current were also recorded along with phase enabling COP to be determined from power calculations.

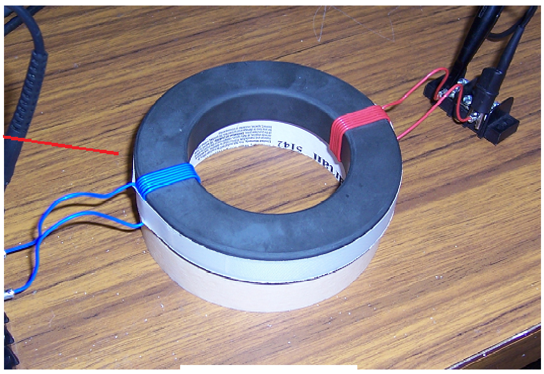

Figure 1

## 3. Magnetic Domain Model.

Figure 2 shows the simple magnetic domain circuit for a transformer that is loaded by a capacitor C in parallel with a resistor R. These reflect into the magnetic circuit as magnetic components, the resistor appearing as a magnetic inductor $\mathcal{L}=N^2/R$ while the capacitor reflects as a negative reluctance $\mathcal{R}=-\omega^2N^2C$ where N is the secondary turns. These are in series with the core reluctance where flux Φ is driven via the primary current $i_{drive}$ which appears as an mmf generator $U=Ni_{drive}$. In the modification to this model the core appears as a form of transmission line where account can be taken of the propagation time from primary to secondary and vice versa, Figure 3.

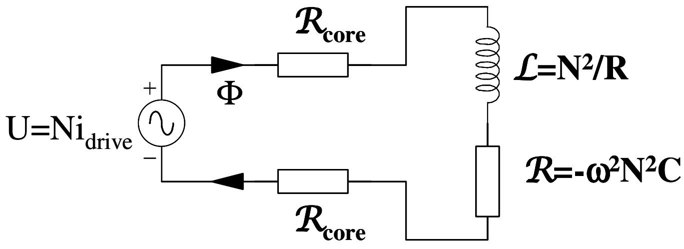


Figure 2.

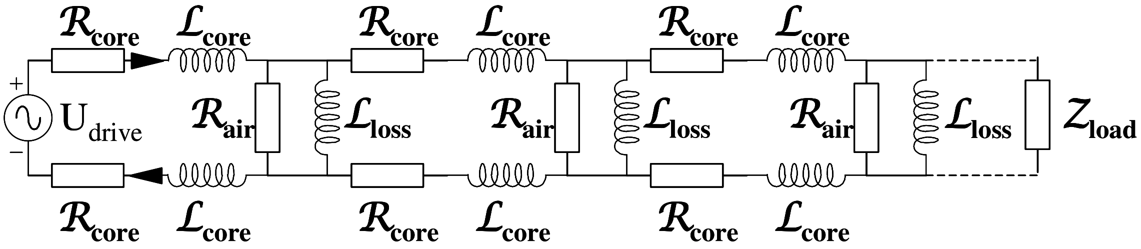


Figure 3.

Here the core reluctance appears as a distributed parameter, along with a distributed magnetic inductor representing the core losses. Also included is the leakage flux shown as distributed shunt air reluctance (actually modelled as distributed inverse reluctance, permeance or magnetic conductance $\mathcal{G}$). Losses in the flux leakage are shown as distributed magnetic inductors (actually modelled as distributed inverse magnetic reactance, magnetic susceptance $\mathcal{B}$). Then, just as the characteristic impedance of an electrical transmission line would be $Z_0 = \sqrt{\frac{R + jX}{G + jB}}$ so the *magnetic* impedance of this line is $\mathcal{Z}_0 = \sqrt{\frac{\mathcal{R} + j\mathcal{X}}{\mathcal{G} + j\mathcal{B}}}$. The propagation velocity is taken as that which pertains at microwave frequency, i.e. $c/\sqrt{\mu_R K}$ where *c* is light velocity, $\mu_R$ is the relative permeability (900 for 3F4 ferrite) and *K* is dielectric constant. Since the dielectric constant is not published, this value is input as a control variable which conveniently allows a quick change to zero propagation delay when *K*=0. It is of interest that the theoretical model gives a best fit to the measurements when *K*=0.7. Losses in the core are accounted for using the published complex permeability for the 3F4 ferrite, which is used to calculate a distributed series reluctance and "magnetic inductive reactance". Since the complex reluctance (expressed as a magnetic impedance $\mathcal{Z}$) for core length *l* and area *A* is $\mathcal{Z} = \frac{l}{\mu_R \mu_0 A}$, and $\mu_R = \mu' - j\mu''$, we find that the distributed reluctance is $\mathcal{R} = \frac{\mu'}{\mu_0 A(\mu'^2 + \mu''^2)}$ and the distributed magnetic reactance is $\mathcal{X} = \frac{j\mu''}{\mu_0 A(\mu'^2 + \mu''^2)}$.

For the distributed shunt permeance (magnetic conductance $\mathcal{G}$) we can use known data on electric transmission lines. The similarity between a balanced line of conductors and one of magnetic conductors is illustrated in Figure 5.

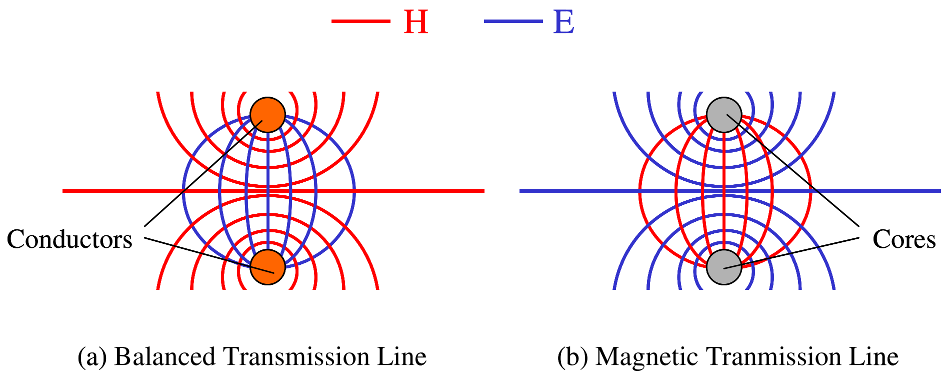


Figure 5.

The equations describing the capacitance between the electric balanced line (a) will be of identical form to those describing the permeance between the magnetic cores in (b). Hence we arrive at the distributed permeance as $\mathcal{G} = \dfrac{3.14\mu_0}{\log_e\left(\dfrac{2D}{d}\right)}$ where $d$ is the core diameter and $D$ is the centre-to-centre distance.

The current model really covers a long thin rectangular core where the impedance is constant along the transmission path, Figure 4.

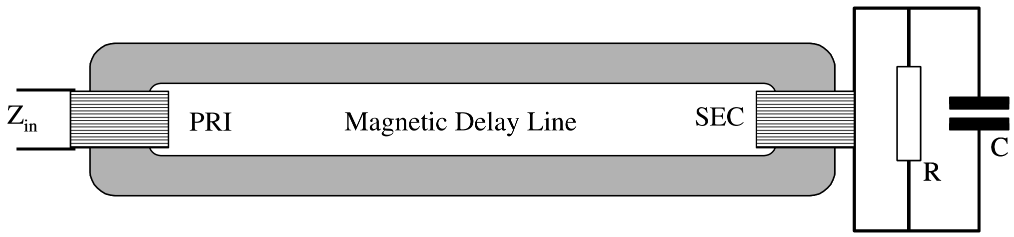


Figure 4.

The circular core can be modelled by multiple sections having different line spacings, but this has not been done yet (the existing model uses 54 spreadsheet columns, extending that to say 10 sections would take the column count to 540!!).

## 4. Comparison between Measured and Calculated Results.

The next page shows a montage of charts comparing measured results with the model, for a 500pF capacitor load shunted with a 10K resistor. Also shown is (a) the effect of removing the leakage flux losses, showing the negative excursion for the real (resistive) part of the input impedance, and (b) increasing the line spacing so as to reduce the leakage flux while keeping the losses present, which also produced the negative excursion.

## 5. Conclusion.

A theoretical model now exists that reasonably predicts the performance of the MDT. This shows that losses associated with leakage flux, thought to be radiation loss, prevent the occurrence of negative input resistance. It is possible that screening the core so as to minimise the flux leakage will allow the negative excursion to appear, leading to a way forward in creating a self oscillating transformer. Minimised flux leakage has been artificially modelled by increasing the line spacing, while keeping the losses present, and this did indeed create the negative resistance, indicating the utility of the screening approach.

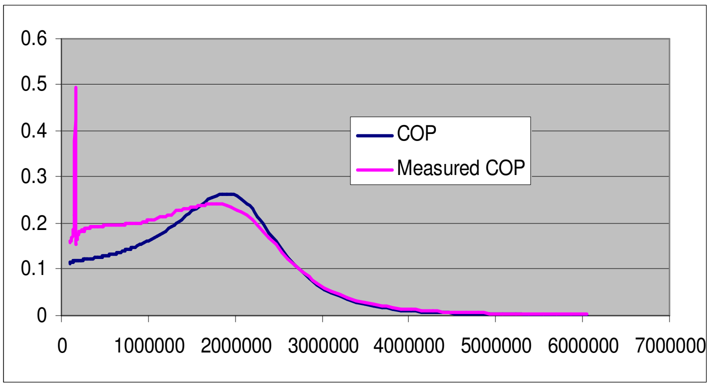
COP
Measured COP
0.6
0.5
0.4
0.3
0.2
0.1
0
0 1000000 2000000 3000000 4000000 5000000 6000000 7000000

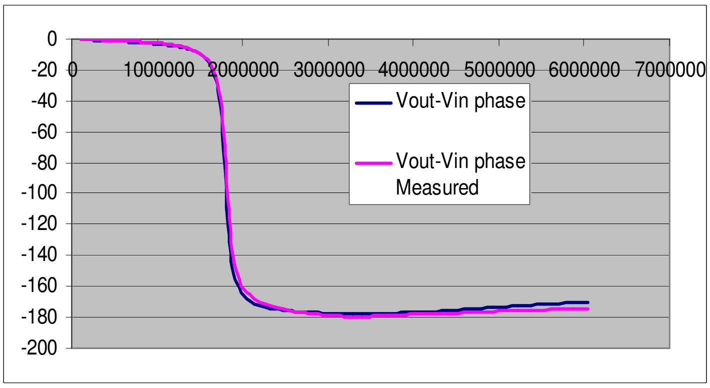
Vout-Vin phase
Vout-Vin phase Measured
0
-20
-40
-60
-80
-100
-120
-140
-160
-180
-200
0 1000000 2000000 3000000 4000000 5000000 6000000 7000000

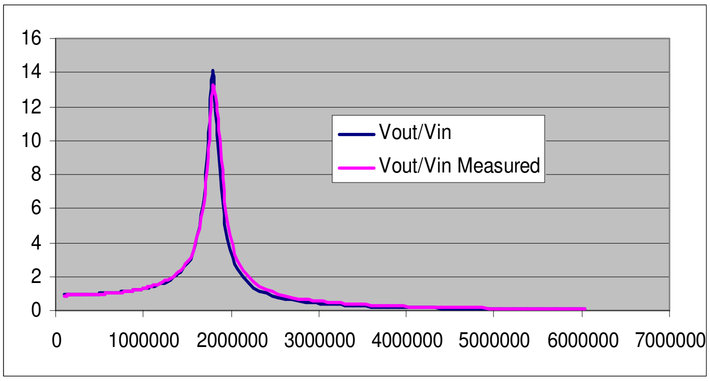
Vout/Vin
Vout/Vin Measured
16
14
12
10
8
6
4
2
0
0 1000000 2000000 3000000 4000000 5000000 6000000 7000000

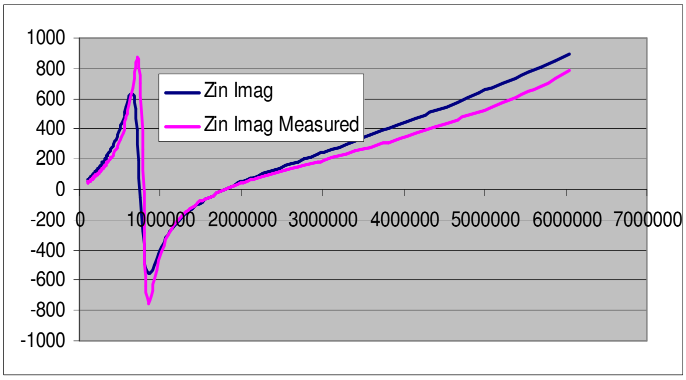
Zin Imag
Zin Imag Measured
1000
800
600
400
200
0
-200
-400
-600
-800
-1000
0 1000000 2000000 3000000 4000000 5000000 6000000 7000000

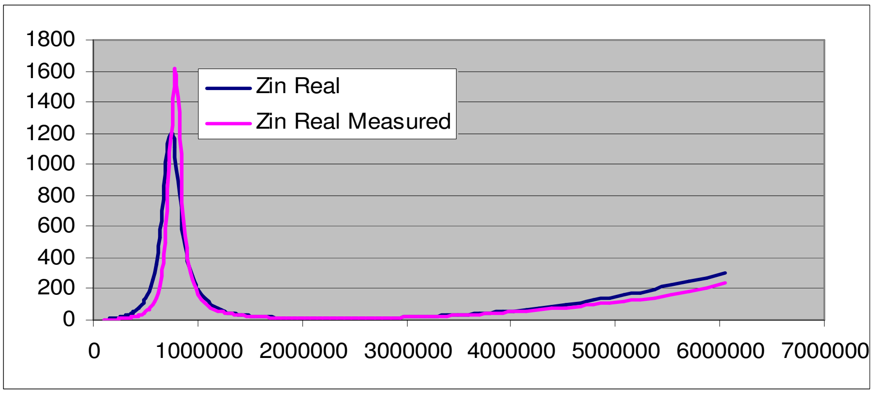
Zin Real
Zin Real Measured
1800
1600
1400
1200
1000
800
600
400
200
0
0 1000000 2000000 3000000 4000000 5000000 6000000 7000000

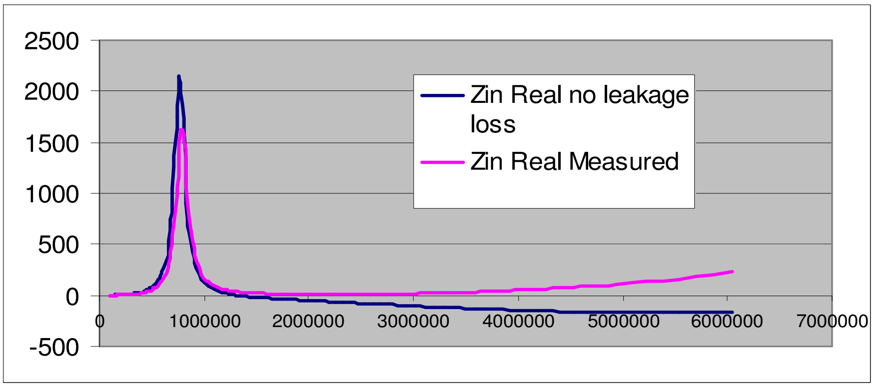
Zin Real no leakage loss
Zin Real Measured
2500
2000
1500
1000
500
0
-500
0 1000000 2000000 3000000 4000000 5000000 6000000 7000000

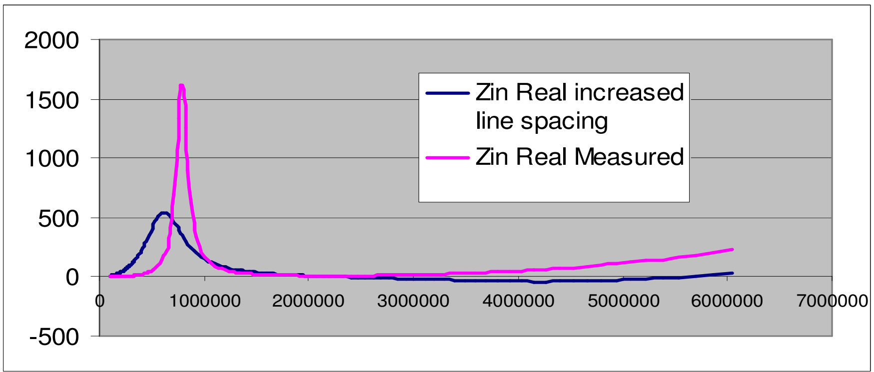
Zin Real increased line spacing
Zin Real Measured
2000
1500
1000
500
0
-500
0 1000000 2000000 3000000 4000000 5000000 6000000 7000000